Sunphotometric observations of the 2001 Asian dust storm over Canada and the U.S.

S. Thulasiraman[1], O'Neill, N. T.[1], Royer, A.[1], Holben, B. N.[2], Westphal, D.[3], L. J. B. McArthur[4]

1. CARTEL, Université de Sherbrooke, Sherbrooke, Québec, Canada
2. GSFC/NASA, Greenbelt, MD
3. Naval Research Laboratories, Monterey, CA
4. Meteorological Services of Canada, Downsview, Ont., Canada

Abstract

Sunphotometry, supported by TOMS imagery and the NRL NAAPs chemical transport model, was used to monitor springtime Asian dust plumes across Canada and the U.S. Comparative analysis between these data sets indicated that the evolution of the dust plume could be inferred at western, mid-western and eastern sunphotometer stations. The dust influence on sunphotmeter monthly statistics is shown to be weak but systematic.

Introduction

Dust storms generated in the Gobi Desert are regular spring time occurrences [*Parunga et al.*, 1994]. *Husar et al.* [2000] reported on the effects of the unusually large Asian dust storm of 1998 and presented a brief history of such events. They noted that Asian dust plumes are regularily transported across the Pacific Ocean. Significant meteorological-scale effects on sunphotometry were observed as early as 1980 by *Shaw* and most recently over the western U.S. during the 1998 dust event [*Tratt et al.*, 2000]. On a climatological scale, *Holben et al.* [2000] noted a significant long term influence of Asian dust on high altitude sunphotometry data collected over Mauna Loa Hawaii.

To our knowledge no study of Asian dust effects has included a pan-North American analysis of sunphotometric data during a major dust event. The object of this paper is to report on the influence of the April 2001 Asian dust event on measurements of aerosol optical depth (AOD) and Angstrom exponent (α) across a number of stations in the west, midwest and eastern regions of the U.S. and Canada.

Methodology

The CIMEL sunphotometers employed in our analysis are part of the AERONET network [*Holben et al.*, 2000]. Seven sites in the northern U.S. and southern Canada (Table 1) were chosen for study in part because they lay within the path of the plume and in part from a geographical sampling strategy which was to observe the dust influence over a pan-North American scale. The Canadian sites are part of the AEROCAN network which is itself a federated member of AERONET. The Roger's Dry Lake site in California is well south of the rest of the stations but was retained to illustrate the southward extent of the measurable optical parameters. Because of a technical problem, the Bratt's Lake CIMEL was not operational so that we employed two 4-channel SP01-A sunphotometers [*anonymous*, 2000]. No operational cloud screening procedure is applied to the output of the SP01; these data were accordingly processed with a cloud screening algorithm similar to that of AERONET[1].

Table 1. Sunphotometer stations whose data was employed in this study

site	Saturna Island, B.C.	Roger's Dry Lake, California	Missoula Nebraska	Bratt's Lake, Sask.	Bondville Illinois	Sherbrooke Québec	Howland Maine
lat.	48° 46' N	34° 55' N	46° 55' N	50° 16' N	40° 03' N	45° 22' N	45° 12' N

[1] However (i) we could not duplicate the triplicate protocol of AERONET and (ii) rather than the empirical second derivative criterion of AERONET we applied a first derivative threshold of $|dAOD/dt| > 0.001$/minute for eliminating couplets of points. This latter filter gives results which are similar to AERONET but more selective at larger optical depths (based on comparisons with independent AERONET data sets) as well as being more attuned to the Bratt's Lake data.

long.	123° 7' W	117° 53' W	114° 4' W	104° 42' W	88° 22' W	71° 55' W	68° 43' W

The CIMEL instruments acquire solar radiances which are transformed into AOD across seven spectral channels (340, 380, 440, 500, 670, 870 and 1020 nm) and, in a separate mode, almucanter sky radiances across four channels (440, 670, 870 and 1020 nm). The sky radiances, along with AOD estimates at the same four channels, are used to perform inversions for particle size distribution and refractive index [*Dubovik et al.*, 2001]. The four-channel, sky radiance data base is distinct from and of significantly lesser sampling frequency than the seven-channel sunphotometric data base. Data reduction on the sunphotometric data base included the cloud screening algorithm of *Smirnov et al.* [2000]. Calculations of α on the sunphotometric data base were performed using the four-channel AERONET definition [*Holben et al.*, 2000].

The aerosol index (AI) product of TOMS (Total Ozone Mapping Sensor) yields images which are proportional to the integrated aerosol concentration [*Hsu et al.*, 1996]. The sign of the index is indicative of the presence of absorbing or scattering aerosols (positive or negative respectively). The fact that TOMS operates in the optically thick UV region ensures a crude form of vertical discrimination in that detectable signals are limited to altitudes above about 1 km.

We also employed NAAPS (NRL Aerosol Analysis and Prediction System) as a means of simulating the dust optical depths (DOD) of the dust event (as well as sulphate and smoke optical depths) over North America [*Tratt et al.*, 2000]. The model which is characterized by a spatial resolution of 1° by 1° and a 6 hour time-step resolution is driven by the meteorological analysis of the Navy Operational Global Atmospheric Prediction System (NOGAPS) [*Westphal,* 2000].

Observations at western, central and eastern sunphotometer stations

Figure 1 shows AI images over North America during the April dust event. The sunphotometer stations listed in Table 1 as well as NAAPS DOD contours (DOD> 0.1) are superimposed on the images. Keeping in mind that the TOMS data suffered from a swath dependent calibration problem which tended to produce banding artifacts along the orbital trajectories [*Seftor,* 2001] the level of spatio-temporal coherence between the NAAPS predictions and the AI image seems quite reasonable.

Figure 2 shows temporal plots of (i) AI, (ii) NAAPS and CIMEL AOD values, and (iii) CIMEL α values for all seven sunphotometer stations. The green vertical lines represent estimates of the dust event duration which we hypothesized as being causally linked (plus or minus a day) to the large DOD peak at Saturna Island and Roger's Dry Lake. The TOMS and NAAPS plume evolution from Figure 1 combined with the temporal station plots of Figure 2 was the basis for this causal interpretation. The systematic low α values associated with larger AOD during the nominal dust events delimited in Figure 2 is a required but not necessarily sufficient DOD condition. Ascribing AOD variations to dust was dependent on this inverse relationship in the presence of relatively large but smooth excursions in AOD and on the supporting evidence offered by the TOMS and NAAPS data. This process was clearly more problematic in the case of the midwest and east coast sites; weaker AOD variations and probable influences by thin homogeneous cloud and/or anthropogenic sources complicated the interpretation.

The end points of the Sherbrooke and Howland dust events were, for example, contaminated by an influx of small aerosols which appear as an increase in the measured values of AOD and α supported by the NAAPS estimation of a sulfate peak. Bratt's Lake was of particular interest given its boundary position on the northern edge of the major plume seen in Figure 1 and given that there was a cloud ceilometer at this site. This latter instrument indicated

thick cloud until the 14th and the afternoon of the 15th and clear conditions on the 16th and the mornings of the 15th, 17th and 18th. Thin mid-altitude structure (from about 3 to greater than 8 km) could be observed in the afternoons of the 17th and 18th. These observations combined with the TOMS and NAAPS information suggested that the ceilometer was most likely insensitive to the dust plume since the cloud screened AOD increased smoothly and significantly on the 16th (while α decreased smoothly and significantly) in the absence of any detectable vertical structure. The vertical structure observable on the 17th and 18th was probably due to inhomogeneous thin cloud and thus the increase in AOD is attributable to thin homogeneous cloud or dust (AODs which survived the elimination threshold of $|dAOD/dt| > 0.001$/min).

Table 2. Geometric mean and standard deviation of the AOD (500 nm, $\tau_g = 10^{<\log\tau a>}$ and $\mu_g = 10^{\sigma(\log\tau a)}$) and the arithmetic mean and standard deviation for α ($<\alpha>$ and $\sigma(\alpha)$) for (a) all of April, (b) DODs, and (c) April with the DODs excluded. $\delta\Delta\tau_g$ is the change in the lognormal standard deviation as viewed on a linear AOD axis.

	(a) April			(b) Dust			(c) April (dust excluded)			April dust influence	
	τ_g	μ_g	N	τ_g	μ_g	N	τ_g	μ_g	N	$\Delta\tau_g$	$\delta\Delta\tau_g$
Saturna	0.137	1.69	332	0.356	1.203	47	0.117	1.46	285	0.020	0.061
Roger's	0.133	1.49	1085	0.242	1.271	158	0.120	1.38	927	0.013	0.030
Missoula	0.137	1.59	338	0.243	1.198	69	0.120	1.52	270	0.018	0.029
Bratt's	0.096	1.36	1923	0.152	1.124	120	0.083	1.33	1192	0.013	0.011
Bondville	0.234	1.40	501	0.281	1.305	83	0.228	1.62	420	0.007	-0.070
Sherbrooke	0.160	1.49	527	0.211	1.270	141	0.145	1.53	386	0.015	0.004
Howland	0.130	1.55	460	0.189	1.352	125	0.114	1.52	336	0.016	0.020
	$<\alpha>$	$\sigma(\alpha)$	N	$<\alpha>$	$\sigma(\alpha)$	N	$<\alpha>$	$\sigma(\alpha)$	N	$\Delta<\alpha>$	$\delta\sigma(\alpha)$
Saturna	0.776	0.433	332	0.286	0.063	47	0.862	0.42	282	-0.086	0.018
Roger's	0.984	0.319	1085	0.556	0.104	158	1.055	0.28	925	-0.071	0.034
Missoula	0.802	0.352	338	0.402	0.112	69	0.916	0.33	268	-0.114	0.021
Bratt's	1.209	0.457	1923	0.689	0.054	120	1.409	0.46	1192	-0.200	-0.004
Bondville	1.013	0.343	501	0.514	0.145	83	1.104	0.28	417	-0.091	0.064
Sherbrooke	0.988	0.348	527	0.543	0.137	141	1.134	0.28	383	-0.147	0.070
Howland	0.921	0.388	460	0.468	0.130	125	1.115	0.27	327	-0.194	0.120

Table 2 shows the optical statistics for the month of April. The dust columns were computed for those points (within the dust event limits of Figure 2) which satisfied (a) AOD >

twice the April average and (b) $\alpha < 0.75$. In addition the AI was required to be at least > 0 while the NAAPS DOD was required to be significantly above the background AOD and not be obscured by contributions from components other than dust. The "dust-excluded" columns were produced by eliminating all dust points from the total data for April. The last two columns are the generic data minus the dust-excluded data and thus represent an estimate of the influence of dust on the statistics of a dust-free month of April. The effect, which is ~ measuremental uncertainty levels [*Holben et al.*, 2000], is nonetheless systematic.

Figure 4 shows the variation of the differential volume distribution (C_v) as a function of the AOD at 1020 nm. C_v represents the total columnar volume of all particles per unit area per unit increment in ln r [*Dubovik et al.*, 2001]. The low scatter of the coarse mode points (C_{vc}) shows that this mode dominates the AOD behavior. Given that the volume weighted average radius (r_v) was found to be only marginally dependent on AOD (correlation coefficient (R) = 0.29) one can state that the DOD variations are largely determined by abundance (integrated number density) changes in the coarse mode. Table 3 shows the generic and DOD statistics of C_v and r_v for April. The lower scatter of C_{vc} relative to C_{vf} in Figure 4 is confirmed for the case of all dust points as well as for the individual stations (with the exception of Missoula). The corresponding slope of C_{vc} versus $\tau_a(1020)$ and the value of r_{vc} are similar to the values obtained by *Dubovik et al.* [2001] for dust off the western coast of Africa (0.67 versus 0.90 and 1.81 $\pm$ 0.27 μm vs 1.90 $\pm$ 0.03 μm respectively).

Table 3 Statistics of microphysical parameters for April and for the DODs of April

	C_{vf}	R	C_{vc}	R	r_{vc}	σ
April (all points)	$.33\tau_a - 0.0015$	0.678	$.77\tau_a - 0.007$	.459	2.4	1.9
DODs, all stations	$.33\tau_a + 0.0004$	0.536	$.67\tau_a - 0.0127$	.950	1.81	0.27
DODs, by station						
Saturna	$-.41\tau_a + 0.1922$	0.650	$.54\tau_a + 0.0339$	.808	1.81	0.05
Roger's Dry Lake	$1.25\tau_a - 0.1115$	0.775	$.53\tau_a + 0.0129$	.970	1.69	0.13

Missoula	$.21\tau_a + 0.0113$	0.976	$.65\tau_a + 0.0027$	.950	2.25	0.30
Bondville	$.33\tau_a + 0.0049$	0.598	$.80\tau_a - 0.0375$	.974	1.91	0.29
Sherbrooke	$.16\tau_a + 0.0100$	0.426	$.36\tau_a + 0.0237$	.844	1.82	0.22
Howland	$.15\tau_a + 0.0156$	0.874	$.64\tau_a - 0.0146$	.996	1.77	0.14

Conclusions

Dust clouds from the April 2001 Asian dust event were tracked across Canada and the northern U.S. using sunphotometry supported by TOMs data and the NAAPs chemical transport model. Comparisons between these data sets indicated that the dust plume evolution could be inferred at all the sunphotometer stations. Optical statistics for April illustrated how the dust influence was weak but systematic and thus that some consideration should be given to spring time dust events in seasonal AOD climatologies. AOD variations during dust events were dominated by coarse mode volume variations which in turn were largely attributable to changes in particle number rather than size (r_{vc} was relatively constant at ~ 1.8 μm).

Acknowledgements

The authors wish to thank NSERC Canada and the CICS as well as David Halliwell (site manager at the Bratt's Lake station) and Dr. Jeannette Vandenbosch (Roger's Dry Lake site PI).

References

anonymous, SP01 Aureole Sunphotometer, User's Guide, CSD, Brunswick, Victoria, Australia, 2000.

Dubovik, O., Holben, B.N., T.F.Eck, A. Smirnov, Y.J.Kaufman, M. D. King, D.Tanre, and I.Slutsker, Variability of Absorption and Optical Properties of key aerosol types observed in worldwide locations, submitted to *J. Atmos. Sci.*, 2001.

Holben, B.N., T.F.Eck, I.Slutsker, D.Tanre, J.P.Buis, A.Setzer, E.Vermote, J.A.Reagan, Y.J.Kaufman, T.Nakajima, F.Lavenu, I.Jankowiak, and A.Smirnov, AERONET - A federated

instrument network and data archive for aerosol characterization, *Rem.Sens.Env.*, *66(1)*, 1-16, 1998.

B.N.Holben, D.Tanre, A.Smirnov, T.F.Eck, I.Slutsker, N. Abuhassan, W.W. Newcomb, J. Schafer, B Chatenet, F. Lavenue, Y.J.Kaufman, J. Vande Castle, A.Setzer, B.Markham, D. Clark, R. Frouin, R. Halthore, A. Karnieli, N.T.O'Neill, C. Pietras, R.T. Pinker, K. Voss, G. Zibordi, An emerging ground-based aerosol climatology: Aerosol Optical Depth from AERONET, *Jour. Geophys. Res.*, **106**, No. D11, 12067-12097, 2000.

Hsu, N. C., J. R. Herman, P. K. Bhartia, C. J. Seftor, O. Torres, A. M. Thompson, J. F. Gleason, T. F Eck, and B. N. Holben, Detection of biomass burning smoke from TOMS measurements, *Geophys. Res. Lett.*, **23**, 745-748, 1996.

Parungo, F., Z. Li, X. Li, D. Yang, and J. Harris, Gobi dust storms and The Great Green Wall. *Geophys. Res. Lett.*, **21**(11), 999-1002, 1994.

Smirnov, A., Holben, B. N., Eck, T. F., Dubovik, O., Slutsker, I., Cloud Screening and Quality Control Algorithms for the AERONET data base, accepted for publication in *Remote Sens. Environ.*, 2000.

Seftor, C, personal communication.

Tratt, D. M., R. J. Frouin, D. L. Westphal, The April 1998 Asian dust event: a Southern California perpective, *J. Geophys. Res,*

Westphal, D. L., Real time applications of a global multi-component aerosol model. Submitted for publication in: *J. Geophys. Res.*, 2000.

Figure Captions

Figure 1; TOMS AI images overlain with NAAPS (> 0.1) DOD contours and showing the seven sunphotometer stations listed in Table 1

Figure 2; temporal variaton as a function of the (GMT) date in April (a) TOMS AI, (b) NAAPS and CIMEL AODs, (c) CIMEL Angstrom exponent. The vertical green lines indicate the estimated extent of the April dust event at each station.

Figure 3; Differential volume (μm^2 / μm^3) for the fine and coarse mode components (solid and open symbols) vs the AOD at 1020 nm.

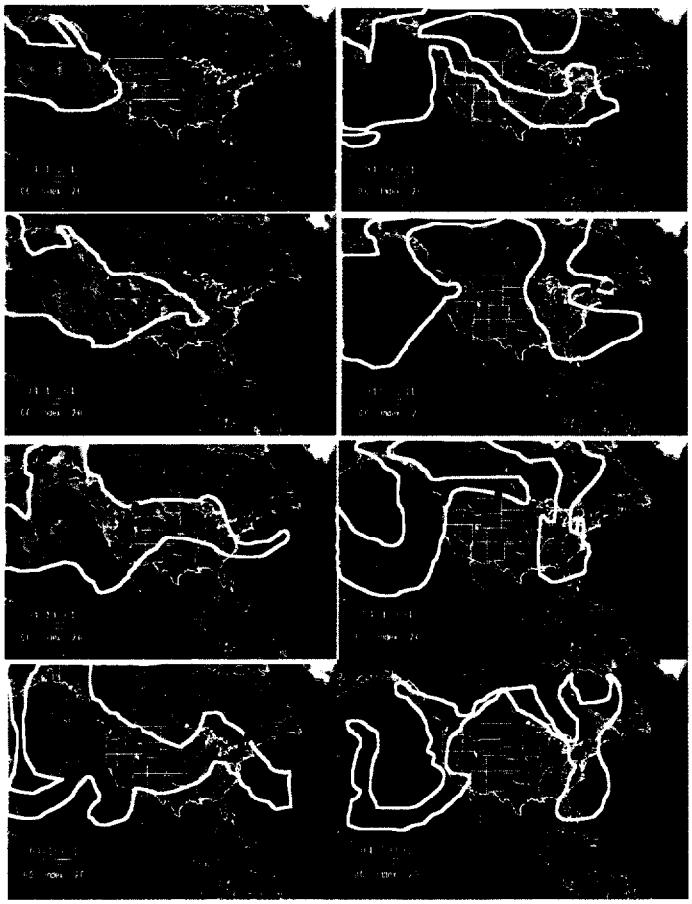

Fig. 1

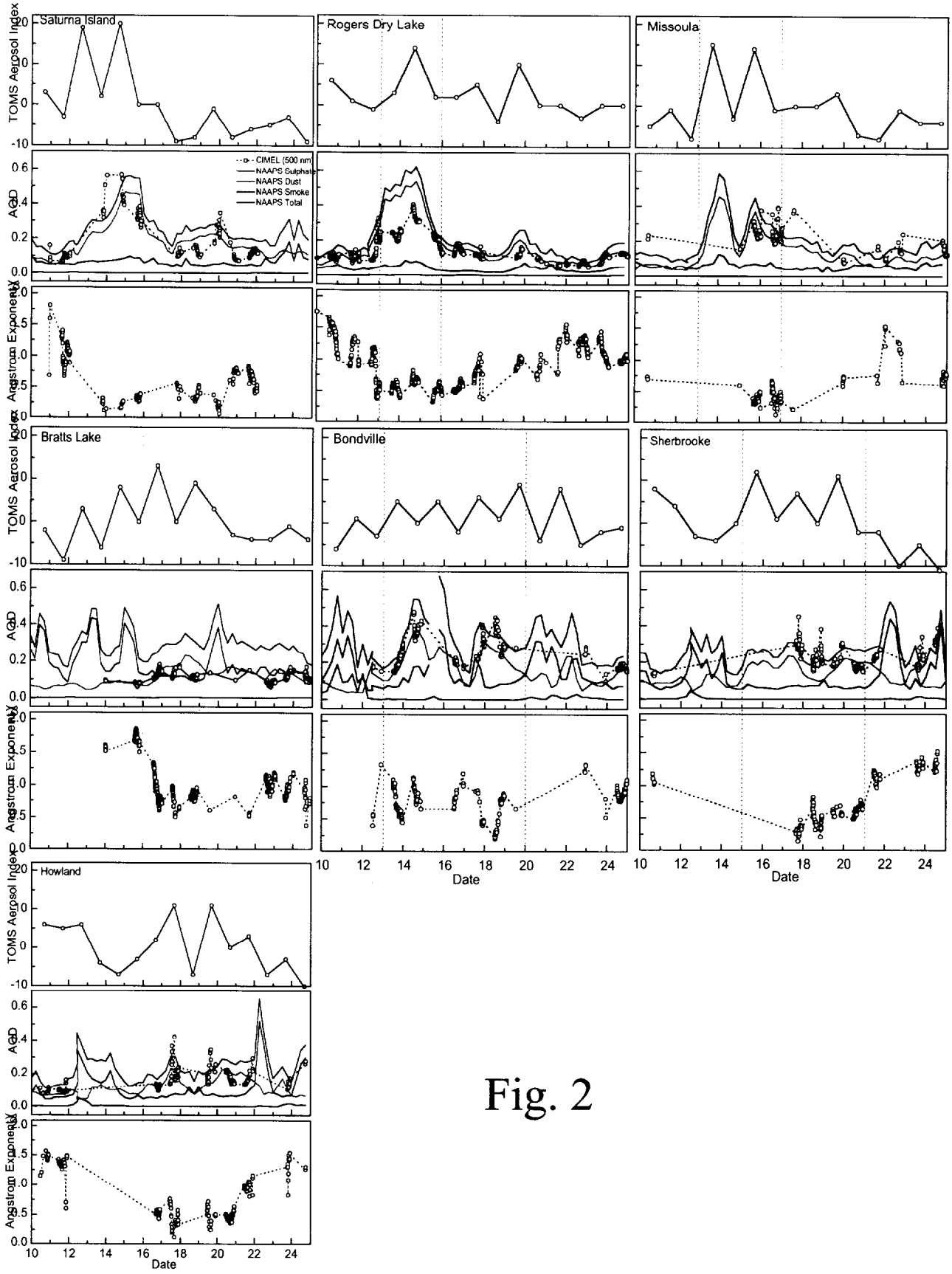
Saturna Island
Rogers Dry Lake
Missoula
Bratts Lake
Bondville
Sherbrooke
Howland
TOMS Aerosol Index
AOD
Angstrom Exponent
CIMEL (500 nm)
NAAPS Sulphate
NAAPS Dust
NAAPS Smoke
NAAPS Total
Date

Fig. 2

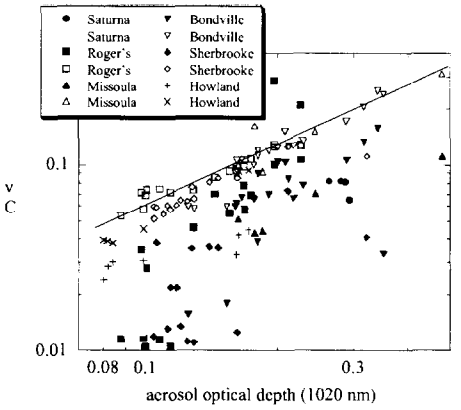
Saturna
Saturna
Roger's
Roger's
Missoula
Missoula
Bondville
Bondville
Sherbrooke
Sherbrooke
Howland
Howland
0.1
0.01
0.08
0.1
0.3
acrosol optical depth (1020 nm)

Fig. 3